21st Australasian Fluid Mechanics Conference
Adelaide, Australia
10-13 December 2018

A Comparison of a Modified Curvilinear Approach for Compressible Problems in Spherical Geometry and a Truly Spherical High-Order Method

M. El Rafei, L. Heidt and B. Thornber

Aerospace, Mechanical and Mechatronic Engineering
University of Sydney, NSW 2006, Australia

Abstract

The dynamics of a variety of compressible physical phenomena such as implosions and explosions occur in spherical geometries. An example application is inertial confinement fusion, where a small capsule containing nuclear material (Deuterium/Tritium mixture) is imploded at high velocities such as undertaken at the National Ignition Facility. In many of those applications, the physics of the flow is greatly impacted by asymmetries generated in the initial stages. Thus numerical methods for these problems must be able to resolve accurately the growth of fundamental instabilities triggered by, for example, non-axisymmetric material properties or initial geometry. These initial asymmetries are so small that numerical generated asymmetries may swamp the physical perturbations.

Here a modified curvilinear approach is presented which reduces asymmetry in spherical meshes by more than an order of magnitude when compared to the standard approaches, even when using Cartesian momenta. This is then compared to a true spherical solver written in spherical co-ordinates and which computes spherical momenta. High-order reconstructions were achieved using a modified spherical fifth-order MUSCL scheme that can be used for both uniform or non-uniform grids. Special attention was carried out in integrating the geometric source terms to avoid situations where a constant pressure and a zero velocity case is not recognized by the solver as a static solution. The performance of the adapted spherical reconstruction was investigated against the modified curvilinear approach and showed that the current approach avoids spurious oscillations at symmetry axis and yields enhanced results where initial physical instabilities are triggered by perturbations smaller than a specified cut off.

Introduction

Finite volume (FV) numerical methods have proved their ability to accurately model flows with strong discontinuities that could be encountered in many compressible physical phenomena in a conservative and oscillation-free way. Compressible solvers based on FV methods rely on computing the fluxes at the cell interfaces from the solution of a Riemann problem which represents a discontinuity in the solution between the left and right states of a specified interface. Those states are reconstructed from the volume-averaged quantities using several reconstruction schemes that are vastly documented in the literature and the reader is referred to [1, 2, 3] for more details regarding FV methods, Riemann solvers and reconstruction techniques. Originally, reconstruction methods were derived for Cartesian domains that are based on uniform grids and little attention was carried out for curvilinear geometries [5]. As a result, Cartesian reconstruction techniques were applied to arbitrary curvilinear grids. One of the ways to achieve that is by using a Jacobian to map the curvilinear grid to a uniform Cartesian numerical grid [4]. However, this approach may not be able to represent accurately some physical phenomena present in the physical grid. Hence, it is more advantageous to use the reconstruction schemes in their original coordinates rather than performing grid mapping and coordinates transformation. As an example, Mignone [6] presented an approach based on inverting a Vandermonde-like linear system of equations with coefficients that vary in space to extend some high-order reconstruction schemes (Piecewise linear method and third-order WENO) to orthogonal curvilinear coordinates. This approach can be used on arbitrary uniform and non-uniform grids and yields less error and reduced spurious oscillations on symmetry axis.

The motivation of this research is to present a true spherical solver that is based on the reconstruction of spherical momenta in spherical coordinates and to compare this approach to a modified curvilinear method that preserves symmetry in spherical grids even though Cartesian momenta are used. More details of both approaches will be introduced in the following sections. The ultimate aim of developing those algorithms is to reduce asymmetries that induce small-scale perturbations which affect the symmetry especially in applications where compressible phenomena occur in spherical geometries. An example application is inertial confinement fusion, where a small capsule is imploded at high velocities. Such implosions should then convert the high velocities to high temperatures and pressures on stagnation, and then achieve ignition conditions. Small perturbations/asymmetries seed instabilities which can substantially reduce the efficiency of the implosion, making fusion ignition impossible. Example instabilities are Rayleigh-Taylor and Richtmyer-Meshkov instabilities [7, 8]. It should be noted that the initial asymmetries are so small that numerically generated asymmetries may swamp the physical perturbations and hence it is crucial to reduce them. This would help in further understanding the growth of the physical instabilities that make fusion ignition more difficult to achieve [9].

Computational Approach and Numerical Methods

The numerical computations were carried out using the in-house code FLAMENCO developed at the University of Sydney. FLAMENCO is a massively parallel compressible multi-block structured solver that involves numerical methods ranging from first-order to fifth-order accuracy. This code was previously used and validated for spherical implosion studies [20] For the multispecies simulations presented within the framework of this study, the spherical solver implemented within FLAMENCO solves the Euler equations to which a transport equation of species mass fraction is added. The mass fraction model suits well the multispecies simulations carried out here since a constant ratio of specific heats (γ) is considered. It should be noted that this model shows a non-physical behaviour represented by spurious oscillations when it is used in cases where γ is variable in the inviscid limit [10]. The volume fraction model or the five-equations model of [11] is adopted for the multispecies simulations carried out using the curvilinear algorithm of FLAMENCO that is based on Cartesian momenta. The reader is referred to [11, 12] for further details about this model. The governing equations are solved using the method-of-lines with the fifth-order MUSCL scheme of Kim [13, 14], to which a modification is implemented in order to ensure a low numeri-

cal dissipation at low Mach number [15]. The Harten, Lax and Leer Contact (HLLC) approximate Riemann solver [16] is used to solve the Riemann problem and the second-order total variation diminishing Runge-Kutta scheme [17] is adopted for time integration.

The true spherical solver implemented in FLAMENCO uses spherical velocity components (v_r, v_θ and v_ϕ), where r, θ and ϕ are the radial, polar and azimuthal directions respectively. This numerical algorithm is devised in such a way that exact cell volumes and face areas are introduced within the governing equations to preserve the required symmetry in a conservative framework. It should be noted that the vector basis in which the vector components are expressed in spherical coordinates is a local vector basis, which means that the latter has no fixed orientation in space. Hence, additional source terms appear in the momentum equations and these terms should be integrated in the conservative approach. The r, θ and ϕ source terms added to the momentum equations could be written as:

$$S_r = \frac{2P}{r} + \frac{\rho(v_\theta^2 + v_\phi^2)}{r} \tag{1}$$

$$S_\theta = -\left[\rho\frac{v_\theta v_r}{r} - \frac{\cos\theta}{\sin\theta}\frac{\rho v_\phi^2 + P}{r}\right] \tag{2}$$

$$S_\phi = -\left[\rho\frac{v_\phi v_r}{r} + \frac{\cos\theta}{\sin\theta}\frac{\rho v_\theta v_\phi}{r}\right] \tag{3}$$

Furthermore, the fifth-order MUSCL scheme used for variables reconstruction is modified so that it uses spherical coordinates rather than Cartesian transformed coordinates. This modification allows the use of the fifth-order MUSCL scheme on arbitrary uniform and non-uniform grids since the space increment in all spatial directions are taken into account. Hence, the use of a Jacobian to map the curvilinear grid into a uniform Cartesian grid in order to use the original Cartesian formulation of the reconstruction scheme is no more necessary.

In regards to the classical approach where FLAMENCO uses Cartesian momenta on curvilinear grids, two fixes are implemented to reduce the asymmetry that is introduced due purely to numerics. Before going into the details of the new fixes, it should be noted that the curvilinear metrics being used to transform the Cartesian momenta into Spherical momenta are second-order accurate and not exact. Hence, the induced discretization errors could affect the symmetry of the conversion between Cartesian and spherical components. Considering for example the radial direction, the radial cell-centred velocity u_r is made up from the Cartesian components u, v and w in three-dimensions, which represent the velocity components in x, y and z directions respectively. This transformed radial velocity component is analytically perfectly radial but it is not perfectly aligned with the numerical face normal which creates a kind of misalignment and hence could be considered as a source of asymmetry. Moreover, the radial fluxes computed at the cell interfaces are based on face-centred conversions and thus, one could notice that two different methods are used to compute the transformed curvilinear components, one is face-centred and the other is cell-centred. Accordingly, a slight angle difference is introduced which affects the symmetry of the problem as shown in figure 1 where i, j represent the radial and azimuthal directions respectively and F is the Flux at the interface. One fix of this issue is to enforce numerically symmetric velocities in the direction where the flux is computed. In other words, the velocity is enforced to be aligned with the face normal numerically and not analytically. This is made by ensuring that the fluxes in the directions where the flux is not computed are kept to zero values.

Another issue that should be addressed is that when the solution is evolved in time a division by the cell volume is applied. Considering a uniform grid, the ratio between the volume and face area between different cells is ideally identical. However, using coordinates transformation, a second-order estimation of the cell-volume is considered which induces discretization errors and the symmetry of the numerical solution is slightly affected. A second fix of this problem is to ensure that the ratio of the volume to face area is constant in the polar direction where slight changes were observed. This is achieved by taking the mean of the maximum and minimum values of this ratio and fixing this value in the computational cells. This fix introduced a small modification of 0.012% to the ratio of volume to face area. These modifications improve significantly the performance of the curvilinear algorithm and preserve the symmetry of the problem.

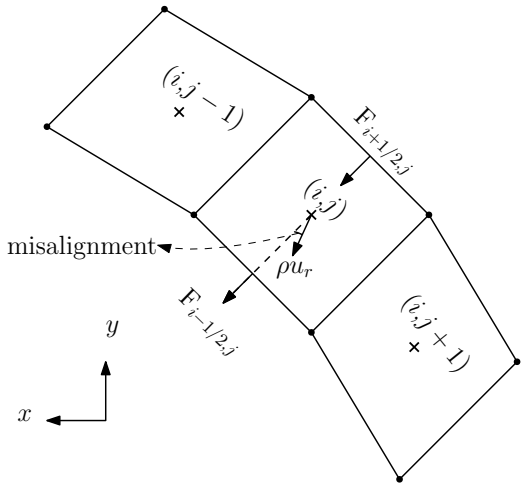

Figure 1: Misalignment between computed face normals and the cell-centred momentum that is made-up from cartesian velocity components using the curvilinear metrics.

In the following, a brief description of the setup used to perform ideal spherical implosions is introduced. The physical model is similar to the one in [18, 19, 20], where the computational domain is split into three regions: the gas region that represents the inner section of the capsule, the shell region which represents the outer shell of the capsule and the source region. The source region is used to incorporate the effect of the shock waves and time-varying physical conditions are prescribed to drive the implosion inwards in time. This is done by applying a global velocity gradient written as $-v_0 r$, where v_0 is a constant and r is the radial position of a computational cell. Low convergence cases characterised by a zero global velocity gradient and high convergence cases with $v_0 = 0.6/ns$ are adopted for the current simulations. More details about the initial conditions used for the spherical implosion setup are represented in table 1.

	Source	Shell	Gas
ρ [g/cm^3]	0.10	1.00	0.05
p [Mbar]	1000	10.00	10.00
v_r [mm/ns]	$-v_0 r$	$-v_0 r$	$-v_0 r$
r [mm]	1.50	1.20	1.0
γ [-]	5/3	5/3	5/3

Table 1: Initial conditions of the spherical implosion case.

In the low convergence case, the shell and gas regions have a zero velocity gradient $-v_0 r = 0$. However, the source region still has a velocity gradient of $0.2ns^{-1}$ applied to it. The perturbation consists of a single spherical harmonic mode that could be described as:

$$\delta R(\theta) = a_0 Y_{l0}(\theta) \tag{4}$$

where a_0 is the amplitude of the harmonic and l is the mode number. It should be noted that a_0 is assumed to be considerably small compared to the wavelength of the harmonic. The computational domain extends from 0.05mm to 1.5mm in the radial direction and from $[0,\pi]$ in the polar or θ direction. A small cut-out is introduced in the region where the origin is located to reduce the computational cost.

Results and Discussions

In this section, qualitative and quantitative analyses of the results given by each algorithm used in FLAMENCO are presented. Qualitatively, a study of a zero-perturbation case is performed which helps in understanding if the interface between the gas and shell regions remains symmetric and free of small-scale numerical perturbations at late time in the simulation. Quantitatively, the perturbation amplitude that is defined as the half of the difference between the maximum and minimum interface radius is presented. A low mode number characterised by $l = 5$ is considered along with a perturbation amplitude of $a_0 = 0.001$. The choice of this amplitude value is based on the fact that small-scale numerical perturbations are more discernable using low mode perturbations. A low convergence case and a high convergence case characterised by a velocity gradient $v_0 = 0.6/ns$ are considered for the computation of the perturbation amplitudes. For more validation, the FLAMENCO results are compared as well to those obtained using PLUTO astrophysical code [21] to understand the performance of our spherical algorithm compared to another well-documented and validated spherical solver. In regards to PLUTO setup, the third-order WENO scheme is used for variable reconstruction and hence a finer grid resolution is adopted in PLUTO (3072×3072) for more consistency in the comparisons. The second-order Runge-Kutta scheme is used for time integration. Details about the grid resolutions adopted in FLAMENCO and the domain sizes are presented in table 2.

	Spherical Solver	Curvilinear Solver
Grid Geometry	(r,θ)	(r,θ)
Domain Size	$[0.05,1.5]\times[0,\pi]$	$[0.05,1.5]\times[0,\pi]$
Resolution	1536×1536	1536×1536

Table 2: Grid geometry, resolution and domain size used for each numerical algorithm implemented in FLAMENCO code.

In terms of computational time, it is important to mention that the curvilinear solver was 1.2 times slower than the spherical solver which induce a considerable reduction in the computational cost. Density contours of a high convergence, zero perturbation case $\left(v_0 = 0.6\ ns^{-1}\right)$ given by the different codes are shown in figure 2. The results given by all solvers are similar in terms of density distribution and shock position. However, the morphology of the small-scale instabilities is significantly different. One could obviously notice that the spherical solver of FLAMENCO remains qualitatively perfectly symmetric with no obvious numerical noise or secondary small-scale instabilities, similarly to the density distribution of PLUTO. In contrast, the interface between the gas and shell regions is overwhelmed with small instabilities that are purely due to numerics using FLAMENCO's curvilinear solver. Quantitatively and based on the maximum and minimum perturbation amplitudes, we estimate approximately a 99.8% reduction of small-scale numerical instabilities using FLAMENCO's spherical solver at very late times. Accordingly, a curvilinear solver is not accurate enough for very low amplitudes as can be seen in figure 2. It is interesting to note that a quantitative comparison between the perturbation heights given by PLUTO and FLAMENCO spherical solver in the zero perturbation case showed that the amplitude of the perturbation was $1/120$ the size of the cell which means that numerically seeded instabilities are negligible. Figure 3 represents a comparison of the perturbation amplitude growth between the different algorithms used in FLAMENCO and PLUTO spherical algorithm. A mode number $l = 5$ and an initial perturbation amplitude $a_0 = 0.001$ are considered for low and high-convergence setups $\left(v_0 = 0\ ns^{-1}, v_0 = 0.6\ ns^{-1}\right)$.

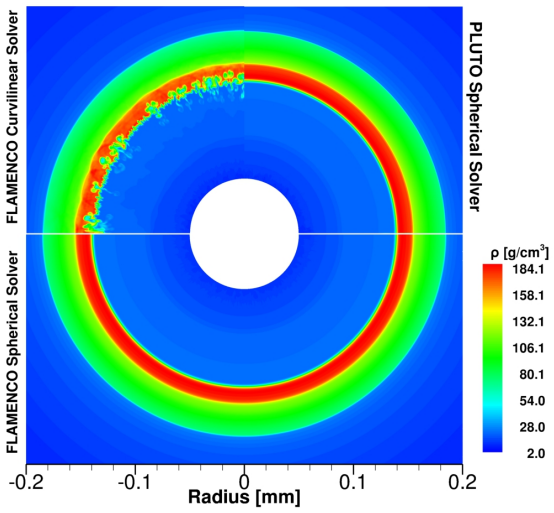

Figure 2: Density contours at $t = 1.2$ ns using the spherical and curvilinear FLAMENCO solver.

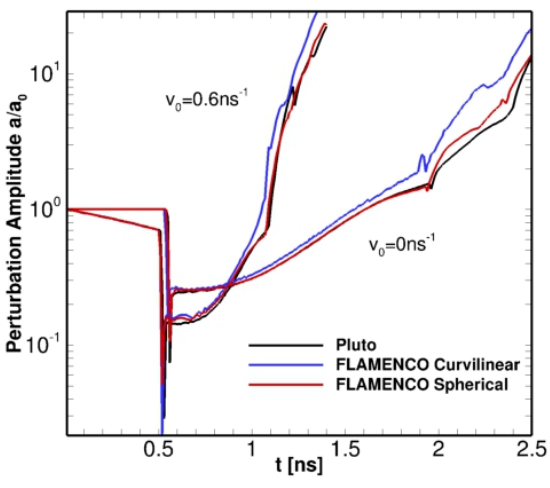

Figure 3: Variation of the perturbation amplitude in time for the low and high convergence cases.

The spherical solver implemented in FLAMENCO is in a very good agreement with the perturbation amplitude trend that is given using PLUTO for both low and high convergence cases until re-shock where FLAMENCO has higher amplitudes than PLUTO in the low-convergence case. FLAMENCO curvilinear solver shows the highest amplitudes compared to the other algorithms, before and after re-shock, which validates in a quantita-

tive way the higher levels of small-scale numerical instabilities that were observed qualitatively in figure 2. The spherical solver of FLAMENCO drastically reduced the numerical perturbation amplitude compared to the classical curvilinear approach which again proves that the curvilinear solver is not accurate enough when solving low perturbation cases.

Conclusions

This paper presented two different numerical algorithms used to compute the dynamics of compressible physical phenomena that occur in spherical geometries such as in inertial confinement fusion cases. The spherical algorithm of FLAMENCO solves the spherical Euler equations and computes spherical momenta that are aligned with the direction of the flux in each spatial direction. Additional Source terms appear in the momentum equations due to the local vector basis used in spherical coordinates. The fifth-order MUSCL scheme was modified in such a way it uses the true spherical coordinates. This is a novelty compared to the classical formulation of this scheme that is adapted for uniform grids. The second curvilinear algorithm computes Cartesian momenta by mapping the curvilinear coordinates into uniform Cartesian coordinates and the symmetry of the spherical problem is preserved by introducing modifications to the estimation of the cell volume and to the alignment of the fluxes with the face normals in each direction. Ideal spherical implosions with a mode number $l = 5$ were considered within this study. The morphology of the small-scale numerical secondary instabilities was quite different between the two algorithms. A zero perturbation case showed that the interface between the gas and shell regions remained perfectly symmetric with no discernable mixing or secondary instabilities when computed using the spherical solver of FLAMENCO. However, significant numerical instabilities were present at the interface using the curvilinear solver. It is interesting to mention that the perturbation amplitude was reduced by 99.8% in the zero perturbation case with FLAMENCO spherical solver. Quantitatively, the perturbation amplitude of our spherical solver had an important agreement with PLUTO [21] spherical solver until re-shock where FLAMENCO had higher amplitudes, whereas the curvilinear solver had significantly larger amplitudes compared to PLUTO. This indicates that the spherical algorithm was able to prevent imminent numerical instabilities that could swamp the physical perturbations. Another important result of this study is that a curvilinear solver is not accurate for low perturbation cases. Finally, the curvilinear solver of FLAMENCO was 1.2 times slower than FLAMENCO spherical solver which presents an important reduction in the computational time for the spherical algorithm.

References

[1] Toro, E.F, Riemann solvers and numerical methods for fluid dynamics: a practical introduction, Springer, 1999.

[2] Harten, A., High Resolution Schemes for Hyperbolic Conservation Laws, *J. Comput. Phys.*, **49**, 1983, 357.

[3] Titarev, V.A. and Toro, E.F. , Finite-volume WENO schemes for three-dimensional conservation laws, *J. Comput. Phys.*, **201**, 2004, 238-260.

[4] Casper, J. and Atkins, H., A finite-volume high-order ENO scheme for two-dimensional hyperbolic systems, *J. Comput. Phys.*, **201**, 62–76, 1993.

[5] Ziegler, U., A semi-discrete central scheme for magneto-hydrodynamics on orthogonal-curvilinear grids, *J. Comput. Phys.* **230**, 2011, 1035-1063.

[6] Mignone, A., High-order conservative reconstruction schemes for finite volume methods in cylindrical and spherical coordinates, *J. Comput. Phys.* **270**, 2014, 784–814.

[7] Rayleigh. Investigation of the character of the equilibrium of an incompressible heavy fluid of variable density. *In Lord Rayleigh, editor, Scientific Papers*, Cambridge University Press, **11**, 1900, 200.

[8] Richtmyer, R.D., Taylor instability in shock acceleration of compressible fluids.*Comm. Pure Appl. Math*, **13**, 1960, 297-319.

[9] Lindl, J., Landen, O., Edwards, J., Moses, E., and NIC Team, Review of the national ignition campaign 2009-2012, *Phys. Plasmas*, **21**, 2014.

[10] Larrouturou, B., How to preserve the mass fractions positivuty when computing compressible multi-component flows, *INRIA Rapports de Recherche No. 1080*.

[11] Allaire, G., Clerc, S. and Kokh, S., A five-equation model for the simulation of interfaces between compressible fluids, *J. Comput. Phys.*, **181**, 2002, 577–616.

[12] Thornber, B., Groom, M. and Youngs D., A five-equation model for the simulation of miscible and viscous compressible fluids, *J. Comput. Phys.*, **372**, 2018, 256–280

[13] Thornber, B., Drikakis, D. , Youngs, D.L. and Williams, R.J.R, The influence of initial conditions on turbulent mixing due to Richtmyer-Meshkov instability, *J. Fluids Eng.*, **654**, 2010, 99-139.

[14] Kim, K.H. and Kim, C., Accurate, efficient and monotonic numerical methods for multi-dimensional compressible flows: Part i: Spatial discretization, *J. Comput. Phys.*,**208**, 2005, 527-569.

[15] Thornber, B., Mosedale, A., Drikakis, D., Youngs, D. and Williams, R.J.R, An improved reconstruction method for compressible flows with low Mach number features, *J. Comput. Phys.*, **227**, 2008, 4873-4894.

[16] Toro, E.F., Spruce, M. and Speares, W., Restoration of the contact surface in the hll-riemann solver, *shock waves*, **4**, 1994, 25-34.

[17] Spiteri, R.J and Ruuth, S.J., A new class of optimal high-order strong-stability preserving time discretization methods, *SIAM Journal on Numerical Analysis*, **40**, 2002, 469-491.

[18] Joggerst, C.C., Nelson, A., Woodward, P., Lovekin, C., Masser, T., Fryer, C.L., Ramaprabhu, P., Francois, M. and Rockefeller, G., Cross-code comparisons of mixing during the implosion of dense cylindrical and spherical shells, *J. Comput. Phys.*, **275**, 2015, 154–173.

[19] Youngs D.L. and Williams R.J.R., Turbulent mixing in spherical implosions, *Int. J. Numer. Methods Fluids*, **56**, 2008, 1597–1603.

[20] Flaig, M., Clark, D., Weber, C., Youngs, D.L. and Thornber,B., single-mode perturbation growth in an idealized spherical implosion, *J. Comput. Phys.*, **371**, 2018, 801–819.

[21] Mignone A., Bodo G., Massaglia S., Matsakos T., Tesileanu O., Zanni C., and Ferrari A., PLUTO: a numerical code for computational astrophysics, *Astrophys J Supplement Series*, **170**, 2007, 228–242.